Tensile Properties of Crystalline Polymers: Linear Polyethylene

M. A. Kennedy,† A. J. Peacock,‡ and L. Mandelkern*

Department of Chemistry and Institute of Molecular Biophysics, Florida State University, Tallahassee, Florida 32306-3015

Received April 4, 1994®

ABSTRACT: The force–length relations of a set of linear polyethylene fractions and polymers having most probable molecular weight distributions, encompassing a wide molecular weight range, have been investigated. The study of these polymers can serve as models for semicrystalline polymers. The polymers were crystallized in such a manner as to develop as wide a range as possible in the values of the independent structural variables that describe the crystalline state. Several important generalizations can be made from this work. The sharpness of the transition from a brittle to ductile type deformation is established, as is its dependence on molecular weight and certain of the other key structural parameters. It is also quite evident that there is no unique force–length curve for ductile deformations. The character of these curves is very dependent on molecular weight. The deformation process cannot be described in terms of changes in crystallographic features. Neither is there any influence of the supermolecular structure. The ultimate properties are found to depend only on the weight-average molecular weight, indicating the importance of the noncrystalline regions. The initial modulus also depends on the noncrystalline region, albeit in a complex manner. The main variables involved here are the crystallinity level and the interlamellar thickness. In contrast, the yield stress depends on the structure of the crystallite and associated regions. Possible mechanisms for yielding are discussed. Different portions of the stress–strain curves are governed by different structural and molecular features, indicating the complexity of the process.

Introduction

The tensile deformation of crystalline polymers, in general, and the polyethylenes, in particular, has been studied extensively.[1-29] However, the molecular and structural basis underlying the deformation process is not as well understood as would be desired. The main reason for this situation lies in the complexity of the structure of a semicrystalline polymer and the variety of independent structural variables that define the crystalline state.[30,31] These variables in turn depend on the molecular constitution and crystallization conditions. To understand properties, therefore, these variables have to be isolated and their individual roles assessed. Methods of isolating these variables, by control of molecular weight and crystallization conditions, have been demonstrated and applied to many properties.[30,32-41] This strategy has also been used in studies of the tensile deformation of the polyethylenes.[42-44] In the present work we continue this approach with a more extensive study of the linear polyethylenes. Here, attention is focused on molecular weight fractions and on samples that have narrow molecular weight distributions. The main objective is to assess the influence of the independent structural variables on the key parameters that describe tensile behavior. For this purpose the present studies have been restricted to one draw rate and temperature. In this respect we complement earlier work. The work here is restricted to the linear polyethylenes. Copolymers need to be treated separately because of structural differences in both the crystalline and noncrystalline regions.[43] Complementary studies involving random ethylene copolymers will be reported shortly.[45] It is not our objective here to develop procedures that yield the highest elongation or greatest modulus. These goals will be achieved eventually with the understanding of the molecular processes that are involved in the deformation.

Experimental Section

Materials. Two different sets of linear polyethylenes were used in this study. The molecular weight fractions were obtained from the Societe Nationale des Petroles d'Aquitane (SNPA). For these samples the M_W/M_N ratios were in the range 1.1–1.2. The other set consisted of polymers that had most probable molecular weight distributions. They were prepared by the method of Kaminsky *et al.*[46] using $(C_2H_5)_2ZrCl_2$ as the catalyst. Details of the molecular weights of the samples are given in Table 1.

Sample Preparation. About 150–160 mg of polymer was placed on a 3.8 × 3.8 cm, 0.127-mm-thick mold that was positioned between aluminum, carbon steel, stainless steel, or cooper plates lined with aluminum foil or on a Teflon sheet of 20.3 and 63.5 μm thickness, respectively. Films were prepared by compression molding in a Carver press at a temperature of about 160 °C and a pressure of $\approx 2.3 \times 10^2$ Pa. The plate system was clamped with binder clips and held, in the molten state, at that temperature and pressure for about 10 min in order to minimize the effect of thermal history. The samples were then subjected to various crystallization procedures, either isothermal or nonisothermal, in order to achieve as wide a range in crystallinity levels as possible for a given polymer.

Nonisothermal crystallization experiments consisted of quickly transferring samples from the melt to one of the following mixtures: dry ice–isopropyl alcohol (*Q* −78 °C); N_2(l)–*n*-pentane (Q −130 °C); ice–water (IWQ); boiling water (*Q* 100 °C). Other samples were allowed to cool to room temperature on a metal grid, in order to allow air flow after they were removed from the Carver press (SCIA). In another procedure the samples were left in the Carver press, with the pressure decreasing with time, and allowed to cool to room temperature at a rate that took approximately 8 h (SCIP).

For the isothermal crystallization experiments, the plates were quickly transferred into a Mylar bag that was then placed in a thermostated bath, preset at a given crystallization temperature maintained at ±0.1 °C. The Mylar bag was used in order to avoid oil contamination from the thermostatic bath.

Characterization. The densities were measured at 23 °C in an isopropyl alcohol–triethylene glycol gradient column that was calibrated with floats of known densities. The degrees of crystallinity on a density basis, $(1-\lambda)_d$, were calculated from the relation given by Chiang and Flory with constants of 1.000 and 0.853 g/cm³ for the density of the crystalline and liquidlike regions, respectively.[47]

† ICI Explosives Canada, Group Technical Center, BePoeil Site, McMasterville, Quebec, Canada J3G1T9.
‡ Baytown Polymer Center, Exxon Chemical Co., P.O. Box 5200, Baytown, TX 77522.
® Abstract published in *Advance ACS Abstracts*, August 1, 1994.

0024-9297/94/2227-5297$04.50/0

Table 1. Molecular and Structural Characteristics of Linear Polyethylene Samples

M_W	M_W/M_N	cryst cond	$(1-\lambda)_d$	$(1-\lambda)_{\Delta H}$	α_a	α_b	α_c	superstructure	deformn
				A. Fractions					
23 300	1.16	Q-78	0.80	0.63	0.29	0.13	0.58	b	B
38 000	1.15	Q-78	0.61	0.39	0.40	0.16	0.44	b	T
		Q100	0.70	0.60	0.23	0.14	0.63	b	B
		100	0.72	0.74	0.21	0.06	0.73	g	B
68 700	1.15	Q-78	0.59	0.49	0.43	0.13	0.44	a	B
		Q100	0.68	0.49	0.36	0.13	0.51	a	D
		110	0.77	0.63	0.34	0.08	0.58	d	T
		120	0.79	0.71	0.23	0.06	0.74	d	T
		129	0.85	0.70	0.25	0.06	0.69	g	B
		129[a]	0.85	0.67	0.30	0.03	0.67	g	B
96 000	1.14	Q-78	0.61	0.50	0.40	0.15	0.45	b	D
		Q100	0.64	0.47	0.38	0.09	0.53	a	D
		120	0.78	0.77	0.23	0.12	0.65	d	T
		129.3	0.82	0.70	0.19	0.03	0.77	g	T
		129.3[a]	0.84	0.73	0.26	0.08	0.66	g	T
115 000	1.15	Q100	0.63	0.47	0.33	0.13	0.54	b, c	D
142 000	1.41	Q-78	0.57	0.41	0.46	0.19	0.35	b, c	D
		Q100	0.61	0.49	0.37	0.17	0.46	c	D
		130[b]	0.64	0.60	0.26	0.08	0.66	g	T
316 000	1.43	Q-78	0.54	0.44	0.52	0.09	0.39	b	D
		Q100	0.68	0.45	0.44	0.13	0.41	c	D
		130[b]	0.71	0.43				g	T
911 000	1.14	Q-78	0.53	0.40	0.48	0.13	0.39	c	D
				B. Most Probable Molecular Weights.					
40 000	1.88	Q-130	0.76		0.28	0.12	0.60	c	B
		Q-78	0.75		0.25	0.11	0.64	b	B
		Q-78	0.76		0.30	0.14	0.50	b	B
		IWQ	0.75		0.31	0.17	0.52	b	B
		110	0.88		0.28	0.04	0.68	c	B
71 000	2.22	Q-78	0.70		0.29	0.16	0.55	a	D
		IWQ	0.70		0.32	0.15	0.53	b	D
		Q100	0.74		0.25	0.11	0.64	c	D
		SCIA	0.81		0.19	0.06	0.75	d	B
		110	0.85		0.17	0.06	0.77	d	B
		SCIP	0.87		0.15	0.04	0.81	g	B
		120	0.86		0.17	0.06	0.77	g	B
139 000	2.30	Q-78	0.69		0.40	0.16	0.44	c	D
		IWQ	0.68		0.38	0.16	0.46	c	D
		Q100	0.76		0.29	0.16	0.55	b	D
		SCIA	0.80		0.26	0.10	0.64	c	D
		SCIP	0.86		0.18	0.08	0.74	g	T
		125	0.91		0.20	0.06	0.73	g	T
		130[b]	0.91		0.24	0.06	0.70	g	T
259 000	1.99	Q-78	0.60		0.40	0.21	0.39	h	D
		IWQ	0.59		0.42	0.20	0.38	a	D
		Q100	0.64		0.37	0.16	0.47	a	D
		SCIA	0.69		0.33	0.13	0.54	b	D
		SCIP	0.75		0.30	0.10	0.60	c	D
		130[b]			0.24	0.01	0.75	g	T
351 000	2.25	Q-78	0.59		0.41	0.17	0.42		D
		IWQ	0.57		0.42	0.21	0.37	b	D
		Q100	0.63		0.36	0.17	0.48	b	D
		SCIA	0.70		0.32	0.14	0.54	b	D
		SCIP	0.76		0.28	0.08	0.64	g	D
		130[b]	0.85		0.21	0.08	0.71	g	T

[a] Crystallized for 7 days. [b] Crystallized for 30 days. [c] Crystallized for 60 days.

The heats of fusion were determined with a Perkin-Elmer differential scanning calorimeter (DSC-2B) that was calibrated for temperature and melting enthalpy by using indium as a standard. The polyethylenes, and the indium standard, were prepared for the DSC analysis by weighing 1.5–2.0 mg of the material on a Mettler balance into a preweighed standard aluminum DSC pan. The samples were heated from 47 to 167 °C at a scanning rate of 10 °C/min. The areas of the endotherms were determined by planimetry. The heat of fusion (ΔH_u) was calculated by comparing the area of the sample and the standard. The degree of crystallinity was then calculated by comparison with the heat of fusion of a perfectly crystalline polyethylene, i.e., 289 J/g (69 cal/g).[48]

The fraction core crystallinity, α_c, the liquidlike fraction, α_a, and the fraction of the interfacial region, α_b, were obtained by analysis of the 900–1600 cm^{-1} internal mode region of the Raman spectra. The spectra were obtained with instrumentation that has been previously described.[49,50] The method of analysis is based on the one described by Strobl and Hagedorn,[51] as was further refined in this laboratory.[49,52,53]

The crystalline thickness, L_c, was obtained from the Raman low-frequency acoustical mode (LAM). The instrumentation used, the experimental procedures, and method of analysis that was followed have also been described in detail.[54] The LAM data were analyzed following the methods given by Snyder and co-workers.[55,56] The value of 2.9×10^5 MPa was taken as Young's modulus.[57,58]

The supermolecular structures of the crystallized films were determined from the small-angle light scattering (SALS) patterns. For this analysis, samples were placed between microscope slides and cover glass and immersed in silicone oil in order to avoid surface scattering. The light scattering apparatus was similar to

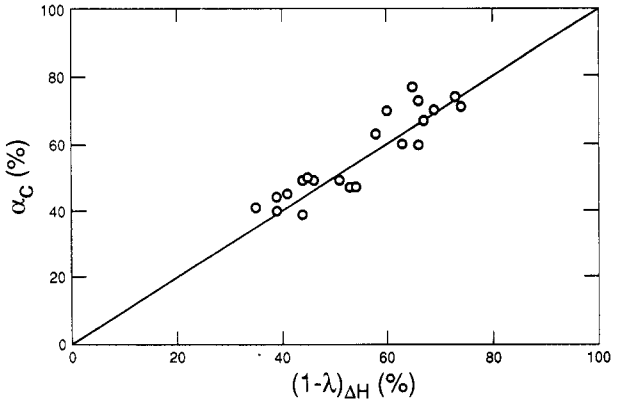

Figure 1. Plot of the degree of crystallinity as determined by Raman spectroscopy, α_c, against the crystallinity level from heat of fusion, $(1 - \lambda)_{\Delta H}$.

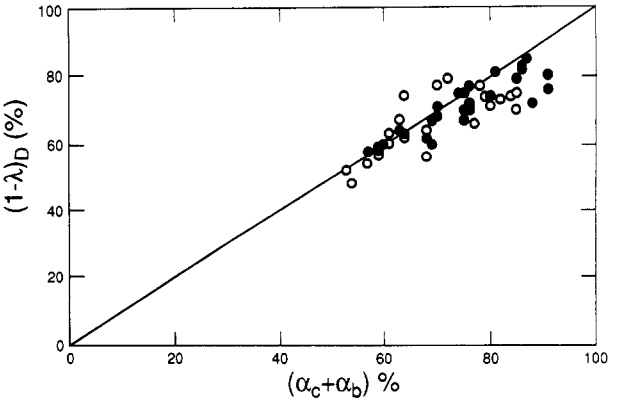

Figure 2. Plot of the degree of crystallinity obtained from density, $(1 - \lambda)_d$, against the sum of $\alpha_c + \alpha_b$: (●) most probable molecular weights; (○) fractions.

the one described by Stein.[59] The terminology used to relate the observed scattering patterns to the supermolecular structure, or morphology, was the same as that defined previously.[32,34] The morphologies labeled a–c refer to spherulitic structures whose development degrades in going from a to c. A d type superstructure refers to lamellae organized into rodlike aggregates; g and h morphologies refer to either rods whose breadth is comparable to their length or randomly oriented lamellae, respectively. The two can be distinguished by some type of microscopic observation. The latter does not represent any well-defined superstructure.

Tensile Measurements. Eight to thirteen dumbbell-shaped samples of gauge length 4 mm, width 1.98 mm, and thickness of about 0.127 mm were cut from the films using a mallet handle die. Fiducial marks were drawn on the specimen to be tested at regular 1-mm intervals. The samples were deformed at room temperature at a draw rate of 2.54 cm/min (1 in./min) using a semimicro tensile tester designed and built in this laboratory.[43] With this instrument molecular weight fractions and other well-characterized samples that are in limited supply can be studied. The initial, or Young's, modulus (E), the yield stress (YS), the ultimate tensile stress (UTS), and the draw ratio after the break (λ_B) were measured as described previously.[43] Mean averages of the different parameters obtained for the 8–13 samples of each film are the actual values reported.

Results and Discussion

The structural characteristics of the samples that were studied are also given in Table 1. The specimens are designated as either B, T, or D depending an whether they were found to be brittle or ductile or in the transition region between the two. The basis for determining these designations will be described shortly. The crystallinity levels were determined by the Raman internal mode α_c and density, $(1 - \lambda)_d$, for all the samples and also by the enthalpy of fusion, $(1 - \lambda)_{\Delta H}$, for the fractions. Most of the polymers were crystallized in such a manner as to develop as wide a range in crystallinity levels as possible. For the complete set of polymers that were studied the crystallinity level based on the density measurements ranged from about 90% to 50%.

It has been reported previously that very good agreement is obtained between $(1-\lambda)_{\Delta H}$ and α_c.[30,60] This concordance is also found with the fractions studied here, as is illustrated in Figure 1. Examination of the data in Table 1 supports previous results that for a given sample $(1 - \lambda)_d$ is significantly greater than $(1 - \lambda)_{\Delta H}$ or α_c.[30,60] However, when $(1 - \lambda)_d$ is plotted against the sum of $\alpha_c + \alpha_b$, a 45° straight line through the origin results, as is illustrated in Figure 2.

The supermolecular structures that develop closely follow the pattern previously described.[32,34] The structures range from well-developed spherulites of the a type to

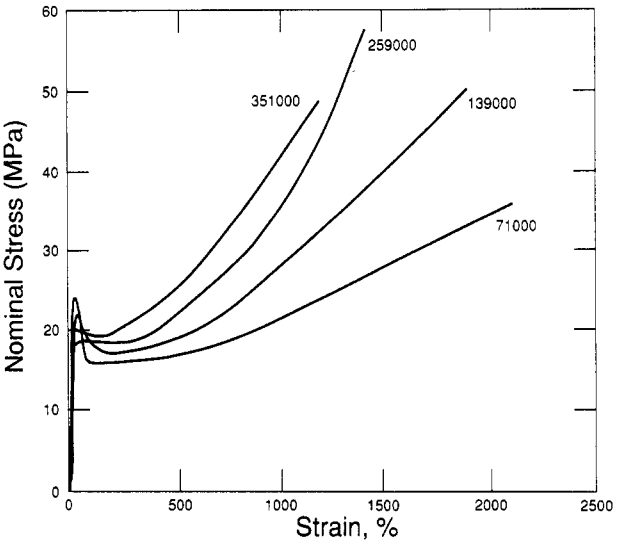

Figure 3. Plot of nominal stress against nominal strain for a series of rapidly quenched linear polyethylenes having most probable molecular weight distributions. The values of M_W are indicated.

randomly arranged lamellae. We note that for the polymer having a most probable molecular weight distribution, M_W = 259 000, random lamellae, all degrees of spherulite structures as well as sheetlike structures have been developed. It will be interesting to note subsequently what influence, if any, the different superstructures have on tensile properties.

We have reported that in a certain molecular weight range linear polyethylene undergoes a sharp transition, from a ductile type deformation to a brittle one ($\lambda_B \simeq 1$) as the crystallinity level is varied.[44] At lower molecular weights the samples are brittle, while at higher molecular weights they are ductile.

Stress–Strain Characteristics. It has been shown that there are no unique stress–strain curves for the linear polyethylenes.[42] In the region of ductile deformation a strong influence of molecular weight has been observed for very polydisperse samples.[4,15,16,42] In Figure 3 the nominal stress is plotted against the nominal strain, in percent, for a series of rapidly quenched samples having most probable molecular weight distributions. All these samples display ductile behavior, and the yield for each is well-defined. However, the yield becomes more diffuse as the molecular weight increases and the value of the yield stress decreases. At the yield point a neck is initiated, becoming established as the stress falls, after which there is a region where the stress does not change very much

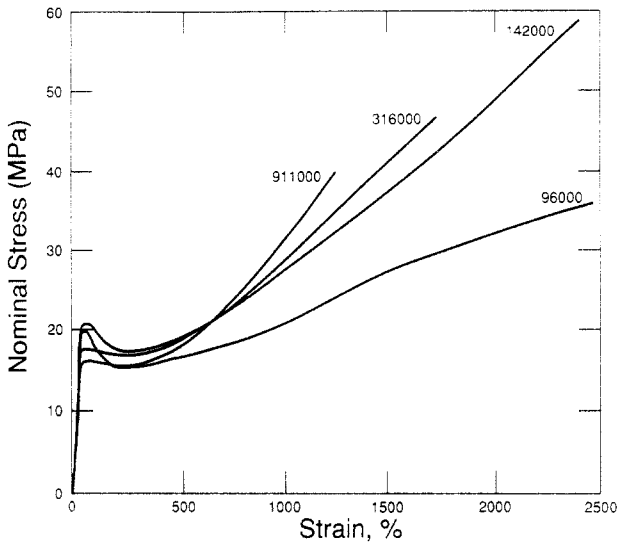

Figure 4. Plot of nominal stress against nominal strain for a series of rapidly quenched molecular weight fractions having indicated values of M_W.

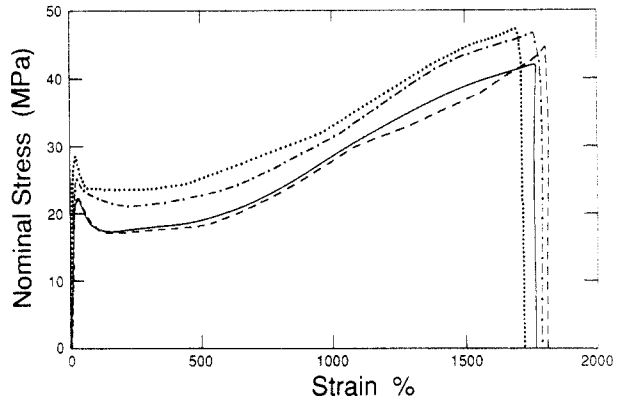

Figure 5. Plot of nominal stress against nominal strain for sample M_W = 139 000, having a most probable molecular weight distribution at different levels of crystallinity: (···) α_c = 0.64; (-·-) α_c = 0.55; (—) α_c = 0.44; (- -) α_c = 0.46.

with elongation and the deformation is inhomogeneous. This region is followed by an upswing in the stress–strain curve, a phenomenon termed strain hardening. With increasing molecular weight the plateau region beyond yield decreases, and the slope of the strain-hardening region becomes steeper. At the high molecular weights the yield is diffuse and poorly defined. A neck is not formed, and the deformation is homogeneous and is governed primarily by the strain-hardening process.

Qualitatively similar results are observed for the molecular weight fractions, as is illustrated in Figure 4. The strain hardening again becomes pronounced with increasing molecular weight. The slopes in this region are qualitatively similar to those found for the most probable molecular weight samples. The polydisperse samples, with broad molecular weight distributions, that were previously studied, showed similar effects when compared on the basis of the weight-average molecular weight.[15,42] Even when considering the molecular weight as the only independent variable, it becomes quite clear that it is not possible to discuss, or select, a typical stress–strain curve.

An example of the influence of the crystallinity level on the stress–strain curves, in the ductile region, is given in Figure 5 for a polymer, M_W = 139 000, that has a most probable molecular weight distribution. This polymer was crystallized under selected conditions so that the core crystallinity levels of the samples studied ranged from 0.44 to 0.64. Over this range in crystallinity levels the stress–strain curves are very similar to one another. All of the curves exhibit a sharp yield. Following yield, the stress remains approximately constant with elongation until the onset of strain hardening. Failure occurs, for these ductile samples, at the same strain, irrespective of the crystallinity level. The main difference between the curves is the decrease in the yield stress with decreasing crystallinity level. Since the shapes of the curves are very similar to one another, a relative vertical displacement of the curves results.

It has already been pointed out that the transition from a ductile to a brittle deformation is very sharp in terms of the crystallinity level.[44] The characteristics of the stress–strain curves of a polymer, M_W = 71 000, which undergoes different types of deformation, by varying the crystallinity level, are illustrated in Figure 6. The two ductile samples, defined by α_c = 0.55 and 0.64, show very

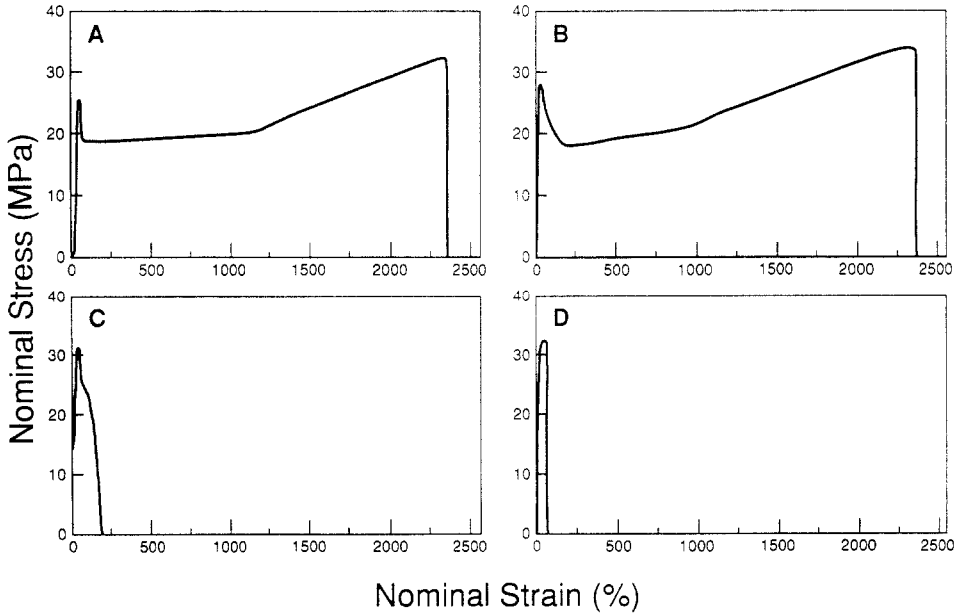

Figure 6. Plot of nominal stress against nominal strain for sample M_W = 71 000 at different crystallinity levels: (A) α_c = 0.55; (B) α_c = 0.64; (C) α_c = 0.75; (D) α_c = 0.81.

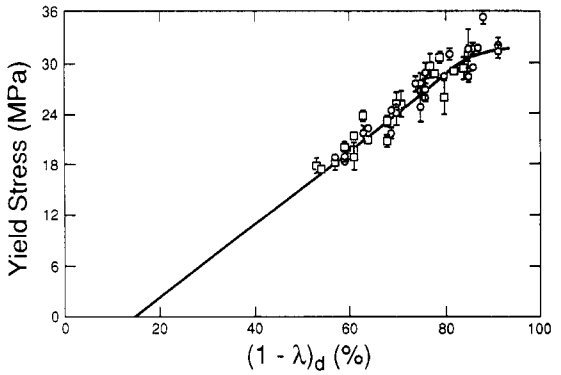

Figure 7. Plot of yield stress against the crystallinity level as determined from the density, $(1 - \lambda)_d$, for all samples studied.

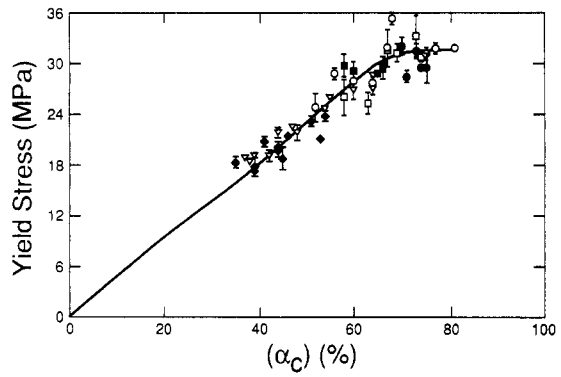

Figure 8. Plot of yield stress against the crystallinity level as determined from the Raman internal modes for all samples studied.

similar stress–strain curves and follow the pattern that we have just discussed. Although the sample $\alpha_c = 0.75$ shows a well-defined yield, there is only a very small deformation region prior to fracture. This sample is classified as being in the transition region since the full deformation range is not achieved. The sample with the highest level of crystallinity, $\alpha_c = 0.81$, also displays a well-defined yield. However, in this case failure occurs just beyond the yield point. This post yield brittle failure is typical of all the brittle samples studied here. Thus, a variety of deformation characteristics can be observed, depending on the molecular weight and the crystallinity level. With this background we can examine specific tensile properties.

Yield Stress. It has been well established, and is apparent from the stress–strain curves of Figures 3 and 4, that the yield stress varies with crystallinity level.[42,43] This dependence is presented in more detail in Figures 7 and 8 for the fractions and the polymers having most probable molecular weight distributions. In these figures the yield stress is plotted against crystallinity levels that are based on either the density or core crystallinity, respectively. The data for the fractions and most probable molecular weight samples fall on the same curve, as do unfractionated samples, that are not plotted here. The two figures display some similarities as well as differences. There is a linear relation at room temperature between the yield stress and crystallinity level in both cases. At the higher crystallinity levels a plateau develops at about 32 MPa. This plateau region is composed of samples that are either brittle or in the transition region. However, such samples are also found in the linear portion of each of the curves, together with all the ductile specimens. Examination of the data in Table 1 shows that there is no direct influence of either molecular weight or supermolecular structure on the magnitude of yield stress. Thus all linear polyethylene samples delineate the same curves when compared on the basis of the same type of crystallinity level. The earlier results of Fulmer and Horowitz[61] for linear polyethylene fractions also follow the plot of Figure 7.

The major difference between Figures 7 and 8 is that when analyzed on the basis of core crystallinity the straight line passes through the origin; i.e., the yield stress is directly proportional to the core crystallinity. On the other hand, the straight line in Figure 7 extrapolates to zero yield stress at a crystallinity level of about 20%. Similar results have been reported for unfractionated, random ethylene copolymers.[43] The differences in Figures 7 and 8 involve the contribution of the interfacial region to the data in Figure 7 but not to that in Figure 8.

The demonstration in Figures 7 and 8 of the strong dependence of the yield stress on crystallinity suggests that the crystallites, or with associated regions, undergo some type of structural change during the yielding process. Two distinctly different mechanisms have been suggested for yielding. Flory and Yoon[62] have proposed that a partial melting–recrystallization process is involved in the deformation process. During deformation an adiabatic heating process takes place.[63–66] When coupled with the applied stress, partial melting and recrystallization should occur.[62,66] The magnitude of the temperature rise has been a matter of some argument.[63–66a–c] Raising the temperature is not a necessary condition for partial melting to take place. Nor does complete melting need to occur, as has been implied.[67,68] The applied stress is adequate by itself. The isothermal melting of a small crystalline region will be followed by recrystallization. The orientation of this recrystallized material will be governed by the stress, and the recrystallization of such a preferentially oriented amorphous system will result in a decrease in the stress.[62]

A similar type process can be inferred from the works of Harrison[69–71] and Gent.[72,73] It has also been inferred from electron microscope studies of deformed polyethylene spherulites that melting occurs in the yield zone.[74] Wignall and Wu[75] have demonstrated by small-angle neutron scattering that partial melting-recrystallization is involved in the complete deformation of linear polyethylene. This result is in accord with the hypothesis put forth by Flory and Yoon.[62] These initial experiments did not, however, establish the elongation at which partial melting was initiated. Subsequent neutron scattering studies have shown that this process starts just beyond the yield points.[76] The neutron scattering studies are limited at present to molecular weights $M_W \cong 7 \times 10^4$. They have not as yet been extended to the very high molecular weights.

Alternatively, it has been proposed that yielding in crystalline polymers, in general, and in polyethylene, in particular, involves the thermal activation of screw dislocations with Burgers vector parallel to the polymer chain direction.[77–79] From this model the dependence of the shear yield stress, τ_y, on the crystallite thickness, L_c, can be calculated. Since detailed theory is given in several places,[77–80] we shall only give an outline here that is sufficient for present purposes.

The free energy, ΔG, required to form a screw dislocation of a Burgers vector, b, located at a distance l from the edge of crystallite of thickness L_c is given by

$$\Delta G = \frac{kb^2L_c}{2\pi}\ln\left(\frac{l}{r_0}\right) - blL_c\tau_y \qquad (1)$$

Here k is a function of the shear modulus of the crystal; b, the magnitude of the Burgers vector has the value 2.54 Å, the c-axis dimension of the polyethylene unit cell; r_0 is

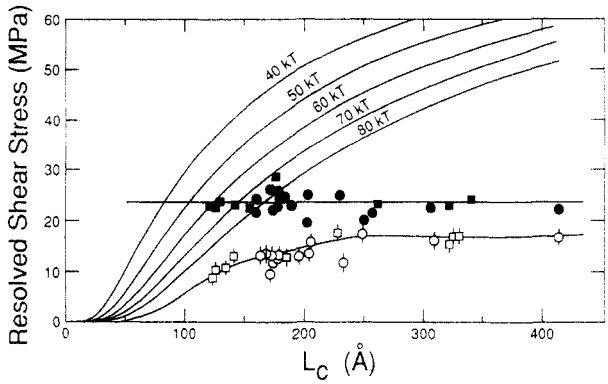

Figure 9. Plot of theoretical and experimental resolved shear stress against crystallite thickness L_c. The values used for ΔG_c are indicated with the appropriate curves. Squares represent fractions and circles samples having most probable molecular weight distributions. The closed symbols represent $\tau_y°$ and the open ones τ_y.

the core radius of the dislocation thought to be on the order of $2b$.[78,79] The critical value of l that is necessary to activate the dislocation, l_c, is obtained from the maximum in ΔG and is given by

$$l_c = kb/2\pi\tau_y \tag{2}$$

The corresponding activation energy for dislocation growth is given by

$$\Delta G_c = \frac{kb^2L_c}{2\pi}[\ln(l_c/r_0) - 1] \tag{3}$$

From eqs 2 and 3 one obtains

$$\tau_y = \frac{k}{4\pi}\left[\exp\left(\frac{2\pi\Delta G_c}{kb^2L_c} + 1\right)\right]^{-1} \tag{4}$$

Equation 4 directly relates the shear yield stress, τ_y, to the crystallite thickness, L_c, and to the temperature through the quantity ΔG_c. ΔG_c is thought to be in the range between 40 and 80 kT.[79]

The tensile yield stress, σ_y, is the measured experimental quantity. It can be converted to the theoretically required shear yield stress, τ_y, needed to apply eq 4, by invoking the Tresca criteria, $\tau_y = \sigma_y/2$.[81] This assumption implies that the yield takes place on crystal planes that are 45° to the tensile axis.[81] Young[78] has made the point that in analyzing experimental data the "crystal" yield stress, $\tau_y°$, defined as

$$\tau_y° = \tau_y/\alpha_c \tag{5}$$

is the appropriate quantity to use in conjunction with eq 4. Following an almost identical theoretical analysis, Crist, however, uses the unmodified τ_y in analyzing experimental data.[79] Since major differences are found, we shall use both τ_y and $\tau_y°$ in analyzing the present set of experimental data.

The quantity τ_y, or $\tau_y°$, is plotted against L_c in Figure 9 for different values of ΔG_c, according to the theoretical relation of eq 4. The parameters that were taken for these calculations, k = 1.486 GPa and b = 2.54 Å, are those that have been suggested.[78] The experimental data for both the fractions and most probable distributions are also plotted. The data cover a range in L_c from 100 to 400 Å. The closed symbols represent $\tau_y°$, while the open symbols are τ_y in the plot. It is evident that the crystal yield stress or reduced yield stress is essentially invariant over this extended range of crystallite thicknesses for the linear polyethylenes. Analysis of these experimental results on this basis does not support the dislocation theory. Plotting the data in terms of τ_y does not improve the agreement with the theory in any significant manner. The data previously reported for unfractionated linear polyethylenes gave results that are very similar to those in Figure 9 when it is recognized that $(1 - \lambda)_d$ is greater than α_c.[30] In analyzing data of this type it is important that homopolymers and copolymers be treated separately. Detailed studies indicate that the data for the copolymers follow a different pattern.[43,45] The previous conclusion that the tensile yield stress was directly proportional to the crystallite thickness was based on a limited amount of data and the erroneous combination of the results for copolymers and homopolymer.[42] The more extensive data presently available indicate the earlier conclusion was incorrect.

Despite the lack of quantitative agreement, the plot in Figure 9 indicates that the dislocation theory predicts the correct order of magnitude of the yield stress. The plot in Figure 8 indicates that in the region of ductile deformation the reduced yield stress is a constant, *i.e.*, independent of the crystallinity level. This observation would appear to implicate the crystallites in this part of the deformation process as has been argued from morphological studies.[7,29,82] On the other hand, the character of the yield, *i.e.*, the shape of the yield region in the stress–strain curve, is very dependent on molecular weight and thus on the crystallinity level. Considering these observations, along with the neutron scattering results, and its theoretical implications, one cannot assign a unique mechanism to the yielding process.

Ultimate Properties. Our discussion of ultimate properties will focus attention on the draw ratio after break λ_B, i.e., the final draw ratio after the failed sample has contracted, and on the ultimate tensile strength. We shall examine the transition from a brittle to a ductile type deformation and the influence of molecular weight, polydispersity, and the structural variables that describe the crystalline state on the ultimate properties. Although the ultimate properties of the polyethylenes have been studied, major attention has not been given to the role of the specific structural variables of interest here.[4,5,9,15–19,22,83,84]

The type of deformation can be characterized by the value of λ_B for a given molecular weight. A brittle sample is defined as one with $\lambda_B \simeq 1$. Higher values of λ_B describe the ductile type deformation. It has been reported that the transition from one type of deformation to the other is very sharp when examined on the basis of the crystallinity level.[44] Figure 10 is a plot of λ_B against the core crystallinity level for the set of samples having most probable molecular weight distributions. Samples with $M_W \leq 40\,000$ are brittle over the accessible range of crystallinity levels. For M_W = 71 000, where the change from one type of deformation to the other is achieved, the sharpness of the transition is clearly demonstrated. Within the experimental error, the sharpness of the transition for M_W = 139 000 can be clearly seen. Although $\lambda_B = 1$ cannot actually be achieved for the two highest molecular weight samples, the data indicate the development of a transition region. The fractions follow a very similar pattern. For these samples the complete transition to brittleness occurs in the range 23 000–38 000. Thus, the embrittlement of the fractions at a lower molecular weight demonstrates a subtle effect of polydispersity.

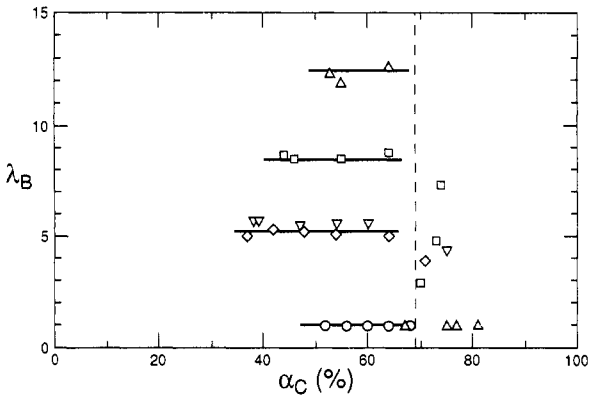

Figure 10. Plot of the draw ratio after break against the level of core crystallinity for polymers having most probable molecular weight distributions: (○) M_W = 40 000; (△) M_W = 71 000; (□) M_W = 139 000; (▽) M_W = 259 000; (◇) M_W = 351 000.

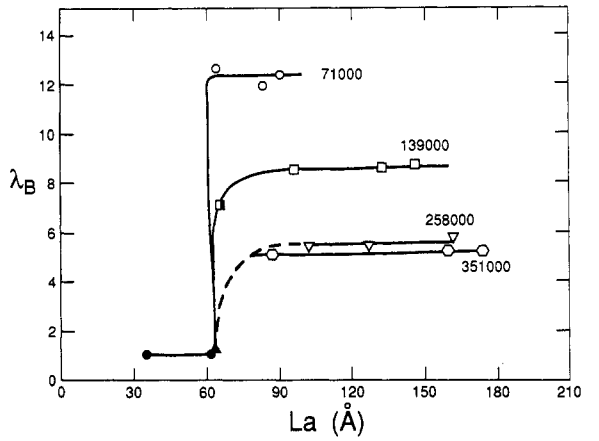

Figure 11. Plot of the draw ratio after break λ_B against interlamellar thicknesses L_a for polymers having most probable molecular weight distributions: (△) M_W = 40 000; (○, ●) M_W = 71 000; (□, ■) M_W = 139 000; (▽) M_W = 259 000; (◇) M_W = 351 000. Open symbols represent the ductile region, filled symbols the brittle region, and half-filled symbols the transition region.

Although we have used the crystallinity level as a convenient variable to describe the different types of deformation, and the transition of one to the other, it is not necessarily the only, or most important, one of concern. Other characteristics, such as molecular weight and interlamellar thickness could also play a significant role in establishing the type of deformation. For example, as is illustrated in Figure 10, M_W = 40 000 is brittle in the range α_c = 52–65%. However, over the same crystallinity range the sample M_W = 71 000 is ductile with λ_B = 12. The higher molecular weight samples behave similarly. The molecular weight fractions follow the same pattern. Therefore, for the same crystallinity level there is a direct influence of molecular weight on the type of deformation that is observed.

On the basis of the Raman LAM data, we can also examine the relationship between λ_B and the interlamellar thickness, L_a. The experimental results are summarized in Figure 11 for the samples having most probable molecular weight distributions. In this figure the open symbols represent the ductile region, the closed ones the brittle region, and the half-filled symbols the transition region. The plots in Figure 11 demonstrate that when the thickness of the interlamellar region is less than about 60–70 Å the samples are either brittle or in the transition region. For samples having greater thicknesses the deformation is ductile for all molecular weights. The transition from one type of deformation to the other is also found to be very sharp when examined on the basis of L_a. The results illustrated in Figures 10 and 11, along with the direct influence of molecular weight, point out that the nature of the interlamellar region is a very important factor in determining whether a sample is brittle or ductile. The crystallite structure is the same in all cases. Careful examination of the data shows that the transition in deformation types is not accompanied by any changes in the supermolecular structure. It has been reported that within narrow limits the transition only varies slightly with the rate of deformation.[44] Thus, the structural features that determine the types of deformation are an inherent part of the crystalline system that is developed.

There are several different reasons that can be advanced for embrittlement. For the set of stacked lamellar crystallites, with which we are concerned, a ductile deformation requires that there be an adequate number of sequences of disordered chain units connecting the crystallites. Furthermore, the number of units involved must be sufficiently large so that each connector is deformable and can sustain large deformations. Put another way, in order to avoid embrittlement, the interlamellar region must possess elements, or chains, that display rubberlike behavior. These connecting chains obviously cannot be straight chains in planar zigzag form.[85,86] The effective number of deformable sequences will be tempered by chain entanglements and interlinking. These factors are sensitive to molecular weight, crystallinity level, and the interlamellar thickness. A plausible assumption for low molecular weight polymers, which are those of concern, is that there is not a sufficient number of disordered sequences connecting the crystallite to transmit the tensile force. Even with an adequate number of such connections, because of the relatively high level of crystallinity involved, the thickness of the interlamellar regions would be expected to be small. Hence, the disordered connecting units would not be able to sustain large deformations. This situation is reflected in the plot of Figure 11, where it is shown that when the interlamellar thickness is on the order of 70 Å or less brittle specimens result.

Another example of the structural sensitivity can be found in an actual crystallizing system.[44] During the course of isothermal crystallization a change from a ductile to brittle deformation occurs with only very small changes in crystallinity as the critical value is exceeded. Either crystallite thickening or further crystallization within the interlamellar region is the cause. In the former case the number of units that can sustain a deformation is reduced. In the latter case although the number of elastic elements will increase, the number of chain units in each is severely reduced. Thus, its rubber elastic properties become severely constrained.

Figure 10 indicates that λ_B is independent of the crystallinity level in the ductile region for a given molecular weight but decreases with increasing chain length. For example, for M_W = 259 000 α_c ranges from 0.39 to 0.60, while λ_B is constant at 5.5 ± 0.1. Similarly, for M_W = 139 000, λ_B is constant in the range 8.5–8.8 over the same range in α_c. The other samples that were studied behave in a very similar manner in that λ_B is independent of the crystallinity level for a ductile deformation.

The influence of the crystallinity level, the crystallite thickness, and the supermolecular structure on λ_B is summarized in Table 2 for a typical set of data. The major features of this tabulation, which are also typical of fractions and the more polydisperse samples,[42] make clear that in the ductile region λ_B is independent of crystallinity

Table 2. Properties in the Ductile Region of Samples with Most Probable Molecular Weight Distributions

crystallinity conditions	α_c	L_c (Å)	superstructure	λ_B
	(a) M_W = 71 000			
Q-78	0.55	175	a	11.9
IWQ	0.53	165	b	12.3
Q100	0.64	192	c	12.6
	(b) M_W = 139 000			
Q-78	0.44	177	c	8.8
IWQ	0.46	175	c	8.5
Q100	0.55	205	b	8.5
SCIA	0.64		c	8.5
	(c) M_W = 259 000			
Q-78	0.39	173	h	5.6
IWQ	0.38		a	5.6
Q100	0.47	234	a	5.4
SCIA	0.54		b	5.5
SCIP	0.60	250	c	5.5
	(d) M_W = 351 000			
Q-78	0.42	183	b	5.3
IWQ	0.37		b	5.0
Q100	0.48	256	b	5.2
SCIA	0.54		b	5.1
SCIP	0.64	220	g	5.0

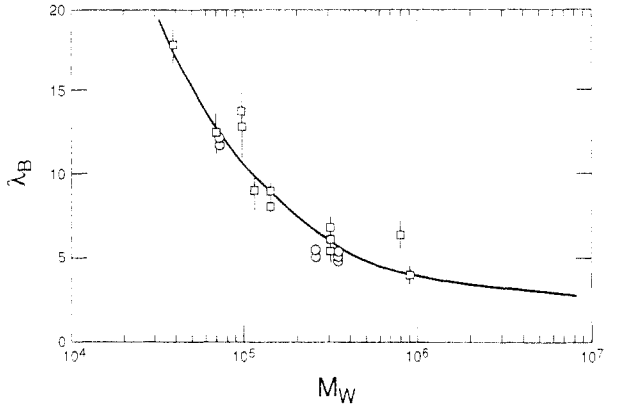

Figure 12. Plot of the draw ratio after break λ_B against log M_W: (solid curve) unfractionated samples from ref 42; (□) fractions; (○) polymers with most probable molecular weight distributions.

level, crystallite thickness, and supermolecular structure. For example, for M_W = 259 000 crystallization conditions were such that a variety of spherulite types, as well as a random organization of lamellae, could be developed. The crystallinity levels range from 0.39 to 0.60, and the crystallite thickness varies from 173 to 250 Å. Nevertheless, λ_B is always 5.5 ± 0.1. For M_W = 139 000, b and c type spherulites are observed; α_c range from 0.44 to 0.64 and L_c from 175 to 205 Å, yet λ_B is a constant. The whole range of spherulitic structures is observed for M_W = 71 000, yet λ_B remains constant at 12.3 ± 0.3 The value of λ_B is thus independent of the structural variables that define the crystalline state. In particular, the same value of λ_B is obtained irrespective of the quality of spherulites that are formed, or in fact, whether spherulites or any type of superstructure develops at all. Thus, we can conclude that in the ductile region λ_B depends only on the weight-average molecular weight of the polymer.

The decrease in λ_B with increasing molecular weight of linear polyethylene has already been reported.[4,22,42] In the present work, however, the molecular weight range is extended and we can also examine the influence of polydispersity. The effect of polydispersity is illustrated in Figure 12. In this figure λ_B is plotted against the weight-average molecular weight. The solid curve in this figure represents the published data for unfractionated, polydisperse linear polyethylene as well as additional unpublished data obtained in our laboratory.[42] Over the molecular weight range $M_W = 5 \times 10^3$–8×10^6 λ_B for the unfractionated specimens decreases from about 18 to 3. The new data points for the fractions, represented by the squares, and the most probable molecular weight samples, represented by the circles, fall on the same curve delineated by the very polydisperse samples. Binary mixtures of the fractions also fall on this curve.[87] The diverse set of samples that is illustrated in Figure 12 make quite evident that, at this deformation rate and room temperature, λ_B depends only on the M_W, irrespective of the details of the chain length distribution. According to the theoretical predictions of Termonia and Smith,[88] the relationship between λ_B and polydispersity should depend on the strain rate. It remains for further investigation to ascertain whether the invariance of λ_B with polydispersity is maintained at other strain rates.

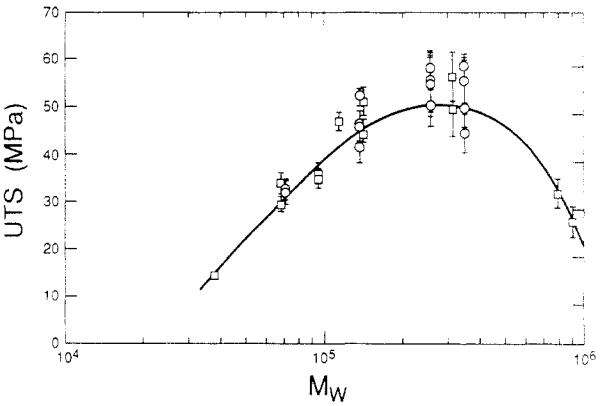

Figure 13. Plot of the ultimate tensile stress against log M_W. Symbols are the same as in Figure 12.

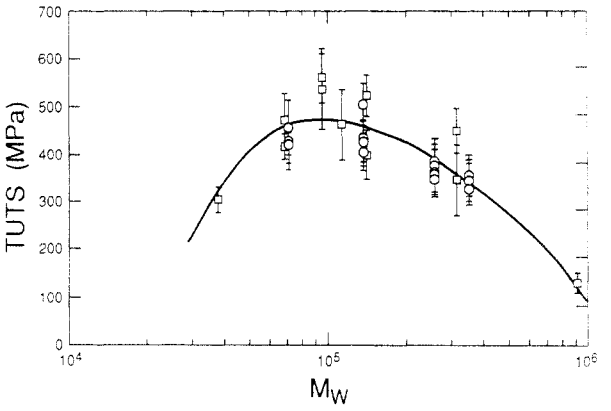

Figure 14. Plot of the true ultimate tensile strength against log M_W. Symbols are the same as in Figures 12 and 13.

Another ultimate property of interest is the tensile stress at break. The ultimate tensile stress in the ductile region, UTS, where the stress is based on the original cross section, is illustrated in Figure 13. It would be of more physical significance to base this stress on the cross section at break. Since this quantity is not available, the approximation is made that the deformation is uniform. With this assumption, the true ultimate tensile stress, TUTS, can be defined as UTS × λ_B. The true ultimate tensile stress is plotted in Figure 14 for the samples in the ductile region. We find that, for either type of analysis, the tensile stress for a sample undergoing a ductile type deformation depends only on its weight-average molecular weight. It does not depend on crystallinity level, crystallite thickness, supermolecular structure, or other elements of structure that describe the semicrystalline state. Both plots give a maximum that is shifted from about 100 000 in Figure 13

to 300 000 in Figure 14. This shift is due to the dependence of λ_B on molecular weight. For molecular weights equal to and greater than 150 000 Figure 14 is similar to that previously reported for unfractionated linear polyethylenes.[42] There is a monatomic decrease from about 400 MPa at the maximum to about 100 MPA for the highest molecular weight sample studied here. The decrease in tensile stress at the lower molecular weights is a reflection of the much reduced strain hardening in this region.

The main conclusion that is reached from these studies is that the ultimate properties in the ductile region only depend on the weight-average molecular weight.[42,89] Concomitantly, however, the crystallinity level continuously decreases with chain length.[31] For M_W about 10^6, α_c is approximately 0.40. One might expect that larger λ_B values would accompany decreasing crystallinity levels; i.e., the system would be more deformable. This expectation is clearly not observed. The crystallographic structure, in terms of the unit cell, is independent of molecular weight. Neither do the general characteristics of the lamellar crystallites change with molecular weight, except in the very high molecular weight range.[90] It is thus evident that deformation in the large strain region, and also possibly after yield, does not involve the crystalline structure alone, if at all. The deformation in this region cannot be treated in the same manner as the plastic deformation of crystals of monomeric substances.[7] It is clearly not crystallographic in nature. For polymers, the total structural system needs to be considered. These factors and the observation that λ_B and UTS depend solely on M_W point out the importance of the noncrystalline interlamellar regions to the deformation process. The importance of the noncrystalline regions in the deformation has been recognized in the past.[13,19,62,83,91] Capaccio *et al.*[19] have pointed out that the topology of the noncrystalline regions is important. The present results emphasize this point.

Flory and Yoon[62] have pointed out that the chain topology initially present in the pure molten polymer will be conserved during crystallization. Such topological features as entanglements, knots, loops, and related structures will be relegated to the interlamellar regions. These types of structures will influence the elastic response of these regions. They depend on the chain length. In particular, the entanglement density increases with M_W. Thus, a connection can be inferred between λ_B, M_W, and the elastic properties of the noncrystalline regions. The decrease in λ_B with increasing chain length can be attributed, among other factors, to the increasing chain entanglement density. Since the entanglements are constrained to reside between the crystalline lamellae, they can act as effective cross-links. Thus, the modulus of this region will increase with molecular weight, and the deformability will concomitantly decrease. The low values of λ_B that are observed at high molecular weights can thus be attributed to the enhanced entanglement density. The response of the interlamellar region to an applied stress has been the subject of a series of theoretical studies aimed at explaining the ultimate properties.[88,92-94]

When developing a detailed analysis of this aspect of the tensile deformation, it is important to note that the presence of spherulites, or how well they are developed, has no influence on λ_B. Therefore, focus that is directed solely on the deformation of spherulites is only of limited aid in understanding the phenomenon. It should also be recalled that spherulites are not a universal mode of polymer crystallization.[34,95]

Initial Modulus. The initial modulus, E, is determined from the slope of the force–elongation curve in the limit of small strain. The initial portion of the force–length curve, about 2–3% strain, is usually reversible. The deformation of the disordered interlamellar region is involved, and the lamellar structure remains essentially intact. Processes such as interlamellar slip, separation, or rotation have been postulated to take place.[7,96] An earlier study with unfractionated linear polyethylene has shown that interpreting the modulus in terms of the basic molecular and structural parameters is complex.[42] A recent study, involving just a few linear polyethylene fractions, has confirmed this conclusion.[79] The specimens being tested here are unique, in that the gauge length is small, 4 mm. Therefore, the absolute values of the moduli cannot be compared with more conventional measurements where the specimen length is usually about 5 times larger.[42,79] The reason for this difference is due to the large radius of curvature, relative to the short gauge length, of the dogbone specimens used here. However, the relative changes in the values of the moduli with changes in structure and molecular constitution are significant.

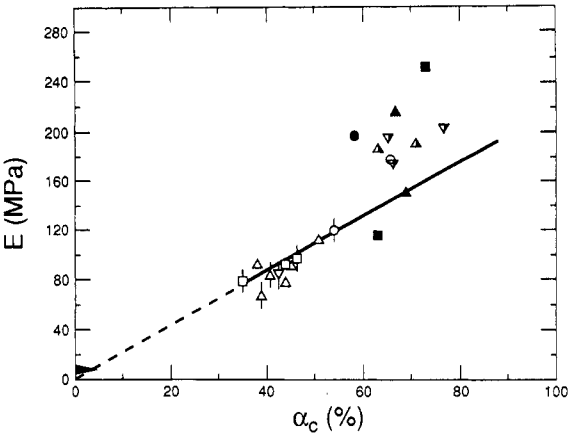

Figure 15. Plot of initial modulus E against core crystallinity level α_c for molecular weight fractions of linear polyethylene: M_W = 23 000 (○); M_W = 38 000 (□); M_W = 68 700 (△); M_W = 96 000 (▽); M_W = 115 000 (◇); M_W = 142 000 (◫); M_W = 316 000 (▲); M_W = 911 000 (▼). Open symbols indicate ductile deformation, closed symbols brittle, and half-filled symbols transitional.

In the earlier study a single plot of E against the density for both linear and branched polyethylenes, resulted in an S-shaped curve.[42] The lower arm consisted of the copolymer data, while the upper one resulted from the linear polyethylene. Attempts to connect the two with a limited data set can lead to misleading conclusions. One of the major concerns is the difference in morphology and lamellar structure between homopolymers and copolymers.

The dependence of E on the crystallinity level, for the samples studied here, is given in Figures 15–18. The two different polymer types that were studied are presented separately, as are two different methods of determining the crystallinity level. We distinguish between the core level of crystallinity, α_c, and the crystallinity level obtained from the density, $(1 - \lambda)_d$. The initial modulus is plotted against the core crystallinity fraction, α_c, for the fractions and the polymers having most probable molecular weight distribution in Figures 15 and 16, respectively. In these, and the ensuing plots, we distinguish by appropriate symbols the ductile, brittle, or transition deformation regions. The general characteristics of the two plots are similar to one another. The initial modulus is directly proportional to α_c up to values of 0.65. In this range of α_c there is approximately a 2-fold increase in E. In both figures there is a great deal of scatter in the data above $\alpha_c \cong 0.65$. At these core crystallinity levels the specimens

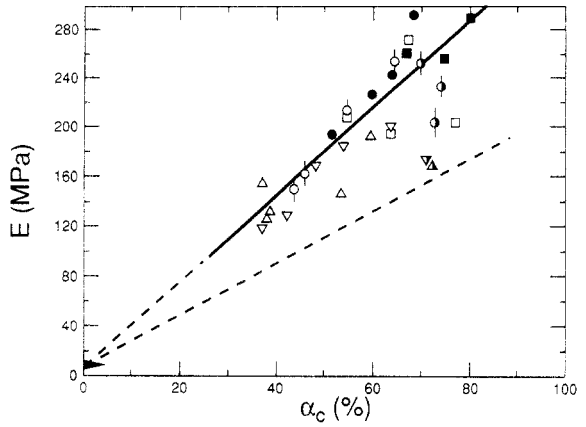

Figure 16. Plot of initial modulus E against core crystallinity level α_c for linear polyethylene with most probable molecular weight distribution: M_W = 40 000 (○); M_W = 70 000 (□); M_W = 139 000 (◇); M_W = 259 000 (△); M_W = 351 000 (▽). Open symbols indicate ductile deformation, solid symbols brittle, and half-filled symbols transitional. Dashed straight line solid from Figure 15.

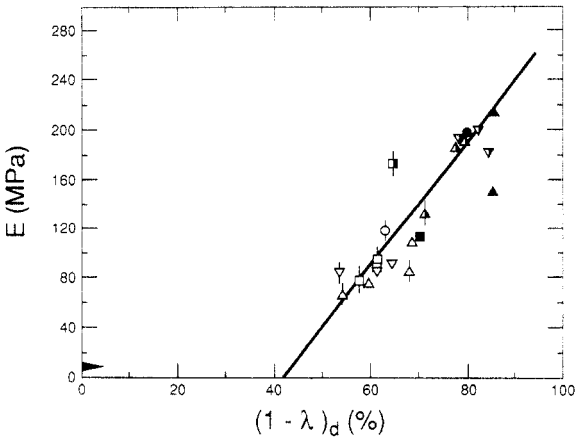

Figure 17. Plot of initial modulus E against crystallinity level determined from density, $(1 - \lambda)_d$, for linear polyethylene fractions. Symbols are the same as in Figure 15.

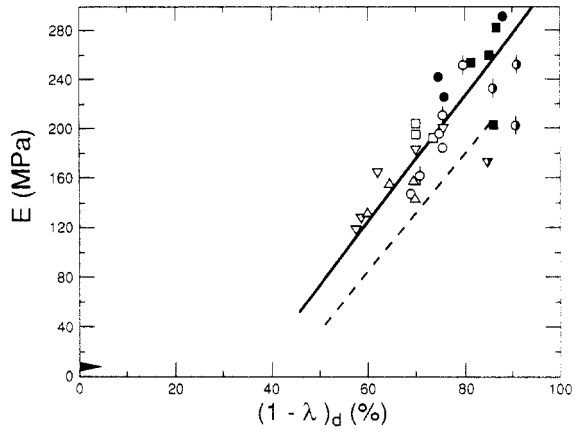

Figure 18. Plot of initial modulus E against crystallinity level determined from density, $(1 - \lambda)_d$, for linear polyethylenes with most probable molecular weight distributions. Symbols are the same as in Figure 16.

are no longer ductile but are either brittle or in the transition region.

Although there is no direct influence of molecular weight on E there is an important indirect influence, by control of the α_c values that can be attained.[30,31] A comparison of the two straight lines in Figures 15 and 16 shows that at the same crystallinity level the moduli values are greater for the samples that have most probable molecular weight distributions. This difference is demonstrated in Figure 16 where the two straight lines are compared. The dashed straight line in this figure is a repeat of the one in Figure 15. There is a subtle, but definite, influence of polydispersity on E. In unpublished work we have found that there is also a direct proportionality between E and α_c for hydrogenated poly(butadienes). However, the slope is reduced relative to that for the linear polymers, thus pointing out the necessity of treating the two types separately.

Similar plots, based on density-measured levels of crystallinity, are given in Figures 17 and 18. In these plots the data points do not scatter as much at the higher crystallinity levels when compared to those of Figures 15 and 16. Each of the two data sets can be well represented by straight lines that, however, do not extrapolate to the origin. It does not make any physical sense for the moduli to vanish at crystallinity levels of 30–40% as the linear extrapolations require. As is indicated by the dashed line in Figure 18, the fractions give somewhat lower values than the samples having most probable molecular weight distributions.

The linear extrapolations to the origin, found in Figures 15 and 16, cannot be precisely valid since a small but finite, rubberlike modulus must exist for the completely noncrystalline sample ($\alpha_c = 0$). This value, as is indicated in the figures, is on the order of 10 MPa.[42,79] Similarly, in Figures 17 and 18 deviations from linearity must occur at about 0.55 so that the values indicated at $(1 - \lambda)_d = 0$ will be approached. At the other end of the scale, as $\alpha_c \rightarrow 1$, the modulus of the completely crystalline polymer should be approached. This value is estimated to be about an order of magnitude greater than has been directly observed using larger size specimens,[42,79] as well as for the values found here. Hence, the linearity would not be expected to extend over the complete crystallinity range. The plots in Figures 15–18, which indicate a continuous increase in the modulus with crystallinity level, demonstrate that the noncrystalline region is a major contributor to the elastic behavior. Since E is determined in the reversible portion of the force–length curve, it would be expected to be governed by the noncrystalline portion. This conclusion is consistent with Figures 15–18. The fact that the data cannot be extrapolated to the extreme values of the crystallinity level in any simple manner does not vitiate this concept. Although it is clear that the degree of crystallinity plays a major role, other structural features may also be involved in determining E. The previous study with unfractionated samples indicate that understanding the initial modulus involves more than specifying the crystallinity level.[42]

Most of the samples that have high E values, equal to or greater than approximately 200 MPa, have g type superstructures.[34] There are, however, major exceptions to this generalization. A set of typical data, relating the morphology to E, are compiled in Table 3. We note, for example, that for M_W = 351 000 and 38 000 although the superstructure type remains constant in each case a significant change take place in the modulus. Conversely, for M_W = 71 000 and 259 000 major changes in the superstructure have been developed for each of the polymers, yet the moduli remain essentially constant. In examining the complete set of data no correlation is found between the supermolecular structure that is present and the value of E.

The relation between E and the crystallite thickness, L_c, is examined in Figures 19 and 20 for the fractions and most probable distribution samples, respectively. Al-

Table 3. Supermolecular Structure and Initial Modulus

M_W	morphology	initial modulus (MPa)
	Most Probable	
71 000	a	206
	b	193
	c	194
139 000	g	235
	g	203
	g	252
259 000	h	131
	a	126
	a	157
	b	148
351 000	b	127
	b	119
	b	165
	b	184
	g	199
	Fraction	
38 000	b	89
	b	116

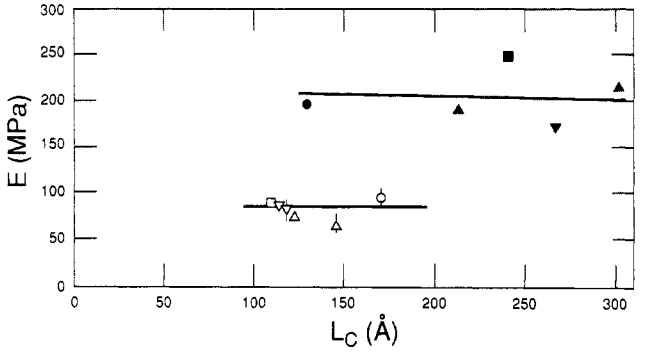

Figure 19. Plot of initial modulus E against crystallite thickness L_c for linear polyethylene fractions. Symbols are the same as in Figure 15.

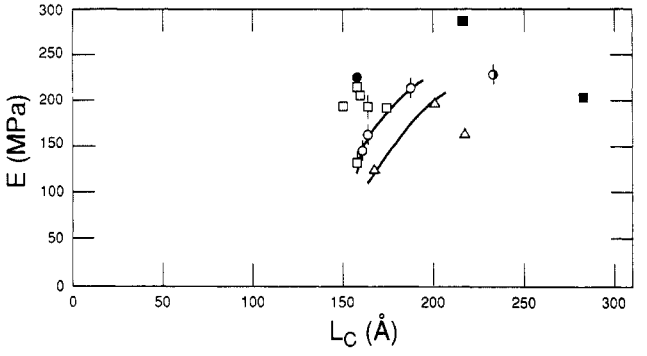

Figure 20. Plot of initial modulus E against crystallite thickness L_c for linear polyethylenes with most probable molecular weight distributions. Symbols are the same as in Figure 16.

though the moduli values for the fractions (Figure 19) fall into two groups, it is quite evident that they do not depend on the crystallite thickness. The higher values for the moduli (the closed symbols) are for the brittle samples and are independent of L_c. The moduli of the ductile samples (open symbols), which have about half the value, are also invariant with L_c. The results for the most probable molecular weight samples (Figure 20) are not as definitive. The moduli of all the brittle samples are also independent of L_c as are the lower molecular weight ductile samples, $M_W \leq 71\,000$. Although the moduli for the higher molecular weight ductile samples scatter somewhat, there is an indication of a slight dependence of L_c.

In a previous study of unfractionated linear polyethylenes the moduli of the very high molecular weight samples were independent of the crystallite thickness.[42]

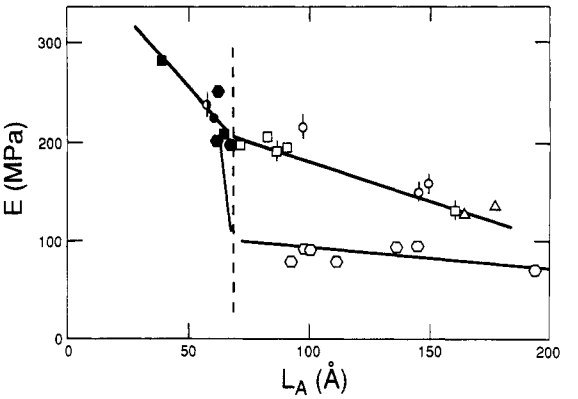

Figure 21. Plot of initial modulus E against thickness of the interlamellar region for fractions and polymers with most probable molecular weight distributions. Most probable molecular weight: $M_W = 40\,000$ (○); $M_W = 71\,000$ (□); $M_W = 139\,000$ (◇); $M_W = 259\,000$; $M_W = 351\,000$. All fractions are represented by ○. Open symbols indicate ductile deformation, closed symbols brittle, and half-filled symbols transitions.

For the lower molecular weights, $M_W = (0.51\text{–}1.5) \times 10^5$, there was, if any, only a slight increase in E with L_c. However, in the intermediate molecular weight range, $(5\text{–}20) \times 10^5$, about a 5-fold increase was observed over the crystallite thickness range of 150–300 Å. The data that is presently available for analysis indicate that both the molecular weight and polydispersity are involved in the dependence of E on L_c.

It has been suggested that the variation of the modulus with crystallite thickness is related to the decrease in the α_1 relaxation transition temperatures below the observation temperature as the crystallite thickness is decreased.[79] Therefore, the modulus of the amorphous component will concomitantly decrease. In turn, the value of E will be affected. Irrespective of any validity to the argument connecting the α_1 transition to the modulus, this transition only changes by about 20–30 °C for the crystallite thicknesses that are involved.[40] Based on loss modulus measurements, the transition occurs in the range 40–70 °C, with the transition temperature being in the range of 60–70 °C for most of the samples. Therefore, ascribing the results to a change in the transition temperature with crystallite thickness is not feasible in this situation. Significant change in the transition temperature only occurs at much smaller crystallite thicknesses, ≤100 Å.[40] These values are not usually within the domain of linear polyethylene and not pertinent to the samples studied here.

Since the initial modulus involves the deformation of the noncrystalline regions, the thickness of the interlamellar reigon, L_a, could be an important factor. To analyze this possibility, E is plotted against L_a in Figure 21. The interlamellar thickness is clearly not a constant and varies from about 40 to 200 Å for the set of linear polyethylenes studied here. In this plot a major discontinuity takes place at about 70 Å. We have already noted that this value of L_a separates the brittle from the ductile specimens. There is a large increase of E as L_a decreases in the brittle region. The large changes in E can be attributed to the lack of deformability of chain units in the thinner interlamellar region and to a substantial contribution from the more rigid crystalline component at the high crystallinity levels that are involved. In contrast, in the ductile region the decrease in E with L_a is fairly modest. In this domain the crystallinity level decreases substantially. Hence, the contribution to E from

the inherent modulus of the noncrystalline region does not change very much.

The reversibility of the deformation at very small strains gives a strong indication that the structure of the interlamellar region has a strong influence on the modulus. In addition to the reversibility, the dependence of the modulus on crystallinity level and interlamellar thickness supports this conclusion. The relatively weak dependence of the modulus on crystallite thickness and its insensitivity to supermolecular structure are consistent with this concept. In the region of small strain one is primarily concerned with a rubber-elastic type deformation, where chain entanglements and other topological features act as effective cross-links. The total system is constrained by the bounding lamellae and their broad basal planes.

Conclusions

In attempting to analyze and summarize these results, it should be recognized that a crystalline polymer of the polyethylene type consists of several distinct structurally different regions.[31] These are the three-dimensionally ordered crystalline regions, the isotropic conformationally disordered, liquidlike regions, and the interfacial regions that connect the two. The trajectories of many of the chains pass through all three regions. Based on theoretical consideration,[96b] it can be concluded that although a high proportion of the chains return to the crystallite of origin only a small portion, about 20% for linear polyethylene, do so adjacently, i.e., are regularly folded.[97] Thus, a structurally disordered interface exists that has no crystallographically defined planes. The relative proportion of the different structural regions that are present depends on both the molecular weight and crystallization temperature and can be varied over wide limits.[31] In high molecular weight linear polyethylene less than half of the system can be considered to be crystalline. The response of the external stress to each of these regions needs to be taken into consideration in analyzing the deformation. There is a set of independent, well-defined, structural variables that, together with the molecular constitution, describe the structure of the crystalline state.[30,31]

Several major features have emerged from the present studies of tensile properties. One is that the general character of the stress–strain curve is very dependent on molecular weight. Hence, it is not possible to consider a typical force–length curve for crystalline polymers, in general, and linear polyethylene, in particular. It it also clear that different portions of the force–length curve are influenced by different structural variables. Hence, a unique analysis that would be applicable to all aspects of the stress–strain curve cannot be given. The interpretation of the results are then complex.

Since we are dealing with a crystalline system, there has been a tendency to focus attention primarily upon the structural changes that can take place within the crystalline regions upon deformation.[7,24,29] Attempts have been made to treat the deformation of the structurally complex polymeric system in analogy with the plastic deformation of metals and other monomeric systems. Polymer crystallites, like other substances, can undergo plastic deformation through several mechanisms. This includes slip, twinning, dislocation motions, and a martensite type phase transition. However, it has yet to be established which, if any, of these processes serves as the structural basis for the deformation of crystalline polymers, and if so, over what portion of the force–length curve they are operative. The experimental results reported here, as well as others,[19,42] make evident that the major mechanisms involved in the deformation of semicrystalline polymers after yield are not crystallographic in origin. The experimental results have shown that the yielding process is subject to several different mechanistic interpretations. Whether these processes operate individually, or in cooperation with one another, is yet to be resolved. Since the interfacial structure is not comprised of regularly folded chains, the postulated unfolding of chains cannot play a significant role in any portion of the deformation.[14] Flory and Yoon have proposed that a partial melting–recrystallization process governs the deformation.[62] As has been indicated, small-angle neutron scattering studies support this concept. Although the general applicability of this process has been established, more detailed information with regard to responses from specific portions of the force–length curve is needed. An important conclusion that can be made from the current studies is that small deformations are governed by the crystallite and associated regions, while at large deformations the ultimate properties depend on the structure of the liquidlike region.

A great deal of attention has also been given to the role of spherulites in the deformation process.[74,96a,98] Spherulitic structures, although quite commonly observed, are not a universal mode of homopolymer crystallization.[34,95,99] Hence, studies that are focused solely on spherulitic properties will, at best, have a limited applicability. Even within this limitation, such a focus could be misleading. Over the wide range of samples and morphologies studied here (see Table 2) no influence could be discerned of supermolecular structure on the deformation.

Haward has shown in an analysis of true stress–strain curves of crystalline polymers that beyond the yield point the results can be described quantitatively by very simple rubber elasticity theory.[100] Put another way, only the deformation of Gaussian coils is involved past yield. The entanglement density (considered as intermolecular cross-links) in the interlamellar region increases with molecular weight. Consequently, the modulus will increase and an enhanced, or steeper sloped, strain-hardening effect will be observed with molecular weight. Furthermore, the increase in effective intermolecular cross-links with chain length will lead to reduced deformability and a decrease in λ_B as is observed. This analysis focuses attention on the rubberlike deformation in the noncrystalline disordered interlamellar region. The strain-hardening phenomenon can be expected to be augmented by strain-induced crystallization.

A theoretical development aimed at explaining ultimate properties, which focuses on the interlamellar region, has been reported in a series of papers.[88,92-94] The model taken for the undeformed semicrystalline polymer is a loose network of disordered entangled chains. The presence of either the crystallites or the domain of the network is ignored. Two rate processes, each governed by an Eyring type activated process, are postulated to be involved in the deformation. One of the activated processes involves the breaking (but not reforming) of van der Waals interactions between disordered chain units. These interactions are introduced to represent the initial stiffness of the system.[92] The other activated process involves slippage of a chain between entanglements. A simulation is then carried out on an array of entanglement points using Monte Carlo methods. The changes in the stress–strain curves with molecular weight that are calculated from this model are qualitatively similar to those observed experimentally. The main features follow the same trends although quantitative agreement is not obtained. It is stated that the stress–strain curves for a low molecular

weight, M_W = 1900, and a high molecular weight, M_W = 250 000, are nearly identical irrespective of whether or not chain slippage is taken into account.

For the calculated examples well-developed yield regions are predicted for all the molecular weights analyzed, even when only the single mechanism of the breaking of van der Waals interactions is taken into account.[92] Since the model that is taken for the calculation consists of a network of coiled, entangled chains, this is a surprising result. The present work, as well as other experimental and theoretical reports,[42,43,78,79] has indicated that the crystallite and associated regions are primarily involved in yielding. Since the results depend on an activated rate process, the particular selection is, in essence, a formal or phenomological matter. The calculations of a sharp yield suggest that the proposed breaking of the van der Waals bonds, which is the only process taken into account in this particular analysis, can also be thought of as representing melting or partial melting. Formally, similar molecular processes are involved. In this way the calculated yield points can be explained that are consistent with the experimental results. The other aspects of the theory, which depend on the influence of temperature and strain rate, are not pertinent to the results reported here.

In this paper we have presented the major features of the tensile properties of the linear polyethylenes and have shown how they depend on the independent structural factors that describe semicrystalline polymers. The relation of these results to current theoretical interpretations is also discussed. A complete molecular understanding of the complete deformation process is clearly not yet at hand. However, these findings should serve as a basis for further developments in this direction.

Acknowledgment. The work was supported by the National Science Foundation Polymer Program DMR 89-14167 and the Office of Naval Research. Their support is gratefully acknowledged.

References and Notes

(1) Sperati, C. A.; Franta, W. A.; Starkweather, H. W. *J. Am. Chem. Soc.* **1953**, *75*, 6127.
(2) Peterlin, A. *J. Polym. Sci.* **1966**, *15*, 427.
(3) Hay, I. L.; Keller, A. *Kolloid Z. Z. Polym.* **1965**, *204*, 43.
(4) Andrews, J. M.; Ward, I. M. *J. Mater. Sci.* **1970**, *5*, 411.
(5) (a) Ward, I. M. *Mechanical Properties of Solid Polymers*, 1st ed.; John Wiley: New York, 1971. (b) Ward, I. M. *Mechanical Properties of Solid Polymers*, 2nd ed.; John Wiley: New York, **1983**.
(6) Andrews, E. H. *Pure Appl. Chem.* **1972**, *31*, 91.
(7) Bowden, P. B.; Young, R. J. *J. Mater. Sci.* **1974**, *9*, 2034.
(8) Perkins, W. G.; Porter, R. S. *J. Mater. Sci.* **1972**, *12*, 2355.
(9) Ward, I. M. In *Ultra-High Modulus Polymers*; Ciferri, A., Ward, I. M., Eds.; Applied Science: London, 1977.
(10) Mead, W. T.; Desper, C. R. R.; Porter, R. S. *J. Polym. Sci., Polym. Phys. Ed.* **1979**, *17*, 859.
(11) Nunes, R. W.; Martin, J. R.; Johnson, J. F. *Polym. Eng. Sci.* **1982**, *22*, 205.
(12) Nielsen, L. E. *Mechanical Properties of Polymer Composites*; Dekker: New York, 1974.
(13) Ichihara, S.; Iida, S. In *The Strength and Stiffness of Polymers*; Zachariades, A. E.; Porter, R. S., Eds.; Dekker: New York, 1983; p 129.
(14) Peterlin, A. In *The Strength and Stiffness of Polymers*; Zachariades, A. E., Porter, R. S., Eds.; Dekker: New York, 1983; p 97.
(15) Steidl, J.; Pelzbauer, Z. *J. Polym. Sci.* **1972**, *38C*, 345.
(16) Capaccio, G.; Ward, I. M. *Polymer* **1974**, *14*, 233.
(17) Capaccio, G.; Ward, I. M. *Polymer* **1975**, *16*, 239.
(18) Capaccio, G.; Crompton, T. A.; Ward, I. M. *J. Polym. Sci., Polym. Phys. Ed.* **1976**, *14*, 1641.
(19) Capaccio, G.; Crompton, T. A.; Ward, I. M. *J. Polym. Sci., Polym. Phys. Ed.* **1976**, *18*, 301.
(20) Peterlin, A. *J. Mater. Sci.* **1971**, *6*, 490.
(21) Truss, R. W.; Clarke, P. L.; Duckett, R. A.; Ward, I. M. *J. Polym. Sci., Polym. Phys. Ed.* **1984**, *22*, 191.
(22) Williamson, G. R.; Wright, B.; Haward, R. W. *J. Appl. Chem.* **1964**, *14*, 131.
(23) Trainor, A.; Haward, R. N.; Hay, J. N. *J. Polym. Sci., Polym. Phys. Ed.* **1977**, *15*, 1077.
(24) Haudin, J. M. In *Plastic Deformation of Amorphous and Semi-Crystalline Materials*; Escaig, B., G'sell, C., Eds.; Les Editions de Physique Les Ulis: Cedex, France, 1982; p 29.
(25) Capaccio, G.; Ward, I. M.; Wilding, M. A. *J. Polym. Sci., Polym. Phys. Ed.* **1978**.
(26) Capaccio, G.; Ward, I. M. *J. Polym. Sci., Polym. Phys. Ed.* **1984**, *22*, 475.
(27) Meinel, G.; Peterlin, A. *J. Polym. Sci., Polym. Phys. Ed.* **1971**, *9*, 67.
(28) Peterlin, A. In *Advances in Polymer Science and Engineering*; Pae, K. D., Morrow, D. R., Chen, Y., Eds.; Plenum: New York, 1972; p 2.
(29) Lin, L.; Argon, A. S. *J. Mater. Sci.* **1994**, *29*, 294.
(30) Mandelkern, L. *Polym. J.* **1985**, *17*, 337.
(31) Mandelkern, L. *Acc. Chem. Res.* **1990**, *23*, 380.
(32) Mandelkern, L. In *Organization of Macromolecules, in the Condensed Phase*; Young, D. A., Ed.; Faraday Society: London, **1979**; Vol. 68, 310.
(33) Mandelkern, L. *J. Phys. Chem.* **1971**, *75*, 3909.
(34) Maxfield, J.; Mandelkern, L. *Macromolecules* **1977**, *10*, 1141.
(35) Mandelkern, L.; Maxfield, J. *J. Polym. Sci., Polym. Phys. Ed.* **1979**, *17*, 1913.
(36) Mandelkern, L.; Glotin, M.; Benson, R. S. *Macromolecules* **1981**, *14*, 22.
(37) Voigt-Martin, I. G.; Mandelkern, L. *J. Polym. Sci., Polym. Phys. Ed.* **1981**, *19*, 1769; **1952**, *65*, 126.
(38) Glotin, M.; Mandelkern, L. *Macromolecules* **1981**, *14*, 1394.
(39) Glotin, M.; Mandelkern, L. *Colloid Polym. Sci.* **1982**, *260*, 182.
(40) Popli, R.; Glotin, M.; Mandelkern, L.; Benson, R. S. *J. Polym. Sci., Polym. Phys. Ed.* **1984**, *22*, 407.
(41) Axelson, D. E.; Mandelkern, L.; Popli, R.; Mathieu, P. *J. Polym. Sci., Polym. Phys. Ed.* **1983**, *21*, 2319.
(42) Popli, R.; Mandelkern, L. *J. Polym. Sci., Polym. Phys. Ed.* **1987**, *25*, 441.
(43) Peacock, A. J.; Mandelkern, L. *J. Polym. Sci., Polym. Phys. Ed.* **1990**, *28*, 1917.
(44) Mandelkern, L.; Smith, F. L.; Failla, M.; Kennedy, M. A.; Peacock, A. J. *J. Polym. Sci., Polym. Phys. Ed.* **1993**, *31*, 491.
(45) Kennedy, M. A.; Peacock, A. J.; Failla, M. D.; Lucas, J. C.; Mandelkern, L., in preparation.
(46) Kaminsky, W.; Hahnsen, H.; Külper, K.; Wöldt, R. *U.S. Patent 4* **1985**, *542*, 199.
(47) Chiang, R.; Flory, P. J. *J. Am. Chem. Soc.* **1961**, *83*, 2057.
(48) Quinn, F. A., Jr.; Mandelkern, L. *J. Am. Chem. Soc.* **1958**, *80*, 3178.
(49) Mandelkern, L.; Stack, G. M. *Macromolecules* **1984**, *17*, 871.
(50) Glotin, M.; Domszy, R.; Mandelkern, L. *J. Polym. Sci., Polym. Phys. Ed.* **1983**, *21*, 285.
(51) Strobl, G. R.; Hagedorn, W. *J. Polym. Sci., Polym. Phys. Ed.* **1978**, *16*, 1181.
(52) Mandelkern, L.; Peacock, A. J. *Polym. Bull.* **1986**, *16*, 529.
(53) Failla, M.; Alamo, R. G.; Mandelkern, L. *Polym. Test.* **1992**, *11*, 151.
(54) Glotin, M.; Mandelkern, L. *J. Polym. Sci., Polym. Phys. Ed.* **1983**, *21*, 29.
(55) Snyder, R. G.; Krause, S. J.; Scherer, J. R. *J. Polym. Sci., Polym. Phys. Ed.* **1978**, *16*, 1593.
(56) Snyder, R. G.; Scherer, J. R. *J. Polym. Sci., Polym. Phys. Ed.* **1980**, *18*, 1421.
(57) Strobl, R. G.; Eckel, R. *J. Polym. Sci., Polym. Phys. Ed.* **1976**, *14*, 913.
(58) Snyder, R. G.; Strauss, H. L.; Alamo, R.; Mandelkern, L. *J. Chem. Phys.* **1994**, *100*, 5422.
(59) Stein, R. S. *New Methods of Polymer Characterization*; Be, K., Ed., Wiley-Interscience: New York, 1964.
(60) Mandelkern, L. In *Comprehensive Polymer Science, Volume 2: Polymer Properties*; Booth, C., Price, C., Eds.; Pergamon Press, New York, 1989.
(61) Fulmer, G. E.; Horowitz, R. H. Proceedings of the VIIth International Congress of Rheology, Gothenburg, Sweden, 1976.
(62) Flory, P. J.; Yoon, D. Y. *Nature* **1978**, *272*, 226.
(63) Vincent, P. I. *Polymer*, **1960**, *1*, 7.
(64) Marshall, I.; Thompson, A. B. *Proc. Roy. Soc. (London)*, **1954**, *221A*, 221,541.
(65) Müller, F. H. *Kolloid-Z.*, **1949**, *114*, 59,118.
(66) (a) Hookway, D. C. *J. Text. Inst.* **1958**, *49*, 292. (b) Maher, J. W.; Haward, R. N.; Hay, J. N. *J. Polym. Sci., Polym. Phys. Ed.* **1980**, *18*, 2169. (c) Toda, A. *Polymer* **1993**, *34*, 2306.

(67) Meinel, G.; Peterlin, A. *J. Polym. Sci., Polym. Phys. Ed.* **1971**, *9*, 67.
(68) Church, H. H.; Lin, J. S.; Porter, R. S. *Macromolecules* **1986**, *19*, 2732.
(69) Juska, T.; Harrison, I. R. *Polym. Eng. Rev.* **1982**, *2*, 14.
(70) Liu, T.; Harrison, I. R. *Polymer* **1987**, *28*, 1861.
(71) Liu, T.; Harrison, I. R. *Polym. Eng. Sci.* **1987**, *27*, 1399.
(72) Gent, A. N.; Jeong, J. *Polym. Eng. Sci.* **1986**, *26*, 285.
(73) Gent, A. N.; Madan, S. *J. Polym. Sci., Part B: Polym. Phys.* **1989**, *27*, 1529,
(74) Phillips, P. J.; Philipot, R. J. *Polym. Commun.* **1986**, *27*, 307.
(75) Wignall, G. D.; Wu, W. *Polym. Commun.* **1983**, *24*, 354.
(76) Wu, W.; Wignall, G. D.; Mandelkern, L. *Polymer* **1992**, *33*, 4137.
(77) Young, R. J. *Philos. Mag.* **1974**, *30*, 85.
(78) Young, R. J. *Mater. Forum* **1988**, *11*, 210.
(79) Crist, B.; Fischer, C. J.; Howard, P. R. *Macromolecules* **1989**, *22*, 1709.
(80) Shadrake, L. G.; Guiu, F. *Philos. Mag.* **1976**, *34*, 565.
(81) Young, R. J. *Introduction to Polymers*; Chapman and Hall: London, 1981.
(82) Galeski, A.; Bartizak, Z.; Argon, A. S.; Cohen, R. E. *Macromolecules* **1992**, *25*, 5705.
(83) Smith, P.; Lemstra, P. J.; Booig, H. *J. Polym. Sci., Polym. Phys. Ed.* **1981**, *19*, 877.
(84) Capaccio, G.; Wilding, M. A. Ward, I. M. *J. Polym. Sci., Polym. Phys. Ed.* **1981**, *10*, 1489.
(85) Keith, H. D.; Padden, F. J., Jr.; Vadimsky, R. G. *J. Polym. Sci., Polym. Phys. Ed.* **1966**, *4*, 267.
(86) Keith, H. D.; Padden, F. J., Jr.; Vadimsky, R. G. *J. Appl. Phys.* **1966**, *37*, 4027.
(87) Failla, M. D.; Mandelkern, L., to be published.
(88) Termonia, Y.; Smith, P. *Colloid Polym. Sci.* **1992**, *270*, 1085.
(89) Warner, S. B. *J. Polym. Sci., Polym. Phys. Ed.* **1978**, *16*, 2139.
(90) Voigt-Martin, I. G.; Mandelkern, L. *J. Polym. Sci., Polym. Phys. Ed.* **1984**, *22*, 1901.
(91) Fischer, L.; Haschberger, R.; Ziegeldorf, A.; Ruland, W. *Colloid Polym. Sci.* **1982**, *260*, 174.
(92) Termonia, Y.; Smith, P. *Macromolecules* **1987**, *20*, 835.
(93) Termonia, Y.; Smith, P. *Macromolecules* **1988**, *21*, 2184.
(94) Termonia, Y.; Smith, P. *Macromolecules* **1988**, *21*, 3485.
(95) Allen, R. C.; Mandelkern, L. *Polym. Bull.* **1987**, *17*, 473.
(96) (a) Young, P.; Stein, R. S.; Kyu, T. *J. Polym. Sci., Part B: Polym. Phys.* **1990**, *28*, 1791. (b) See ref 97 for a summary of the theoretical results.
(97) Mandelkern, L. *Chemtracts: Macromol. Chem.* **1992**, *3*, 347.
(98) Tarin, P. M.; Thomas, E. L. *Polym. Eng. Sci.* **1979**, *19*, 1017.
(99) Allen, R. C.; Mandelkern, L. *J. Polym. Sci., Polym. Phys. Ed.* **1982**, *20*, 1465.
(100) Haward, R. N. *Macromolecules* **1993**, *26*, 5860.